A comprehensive model to evaluate scour formation in plunge pools

E. Bollaert, AquaVision Engineering Ltd, Switzerland

A model to evaluate scour formation downstream of dams is presented and applied to a spillway design case study. The model is physically based, and describes two rock mass failure criteria: progressive break-up of rock joints and dynamic ejection of rock blocks from their mass. It considers the most significant air, water and rock characteristics and their possible interactions. Appropriate model calibration not only provides the ultimate scour depth, but also a reasonable estimate for the time evolution of the phenomenon.

Scour of rock caused by high-velocity jets has been of concern to practicing engineers for some time. A new model has recently been developed to evaluate scour of rock occurring downstream of high-head dams and in plunge pools. Today's most popular evaluation methods are of empirical and semi-empirical nature. They do not fully describe the physical background of the phenomenon. Therefore, the new model was developed based on a parametric description of the main physical processes responsible for scour. The model parameters are chosen to enhance and simplify scour applications, without compromising the basic physical laws they represent.

1. Physical-mechanical processes

The main physical-mechanical processes responsible for scour formation are presented in Fig. 1. A high velocity plunging jet entrains a significant amount of air during its fall and upon impact in the plunge pool. This air-water mixture diffuses through the water depth of the plunge pool, generating a fully turbulent air-water shear layer that interacts with the surrounding pool water. The impact of this shear layer at the water-rock interface results in significant dynamic pressure fluctuations and a lateral deviation of the jet's momentum. Dynamic pressure fluctuations may enter underlying rock joints and progressively break them further open, until the joints encounter each other and the joint network is complete.

Then, instantaneous net pressure differences over and under the formed rock blocks may eject the blocks from the surrounding mass. The blocks are swept into the turbulent flow and may be further broken-up by re-circulation in the plunge pool (ball-milling), or may be transferred to the downstream river. There they are deposited immediately downstream (mounding) or are transported by the river. The present scour model focuses especially on fracturing of rock joints by dynamic water pressure fluctuations inside the joints and on dynamic ejection of the so-formed single rock blocks by net uplift pressures.

Fig. 1. Physical-mechanical processes of rock scour.

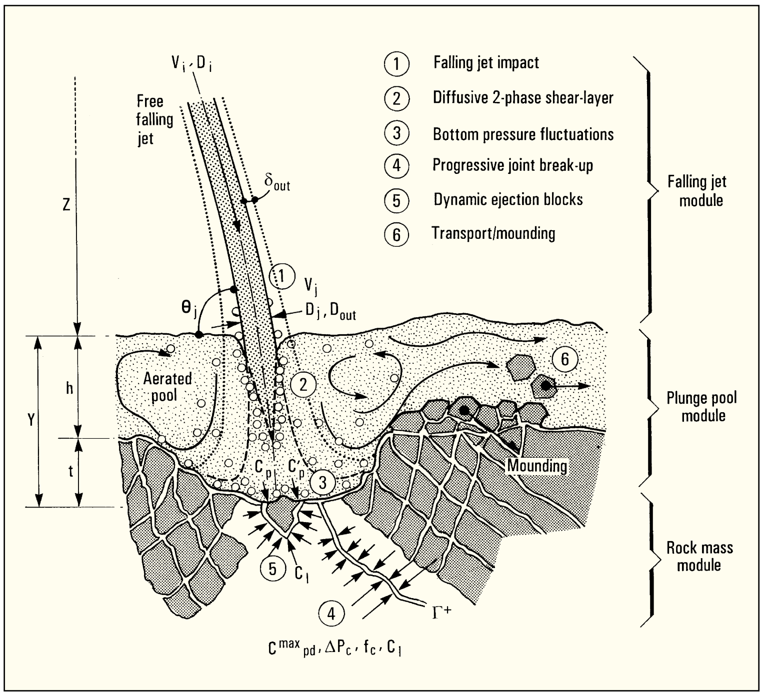

2. Dynamic pressures in rock joints

Dynamic water pressures inside rock joints have been studied both experimentally and numerically at the Laboratory of Hydraulic Constructions of the Swiss Federal Institute of Technology [Bollaert, 2002[1]; Bollaert and Schleiss, 2003[2]].

An experimental facility simulated high-velocity jet impact in a plunge pool and allowed for measuring the dynamic water pressure fluctuations simultaneously at the plunge pool bottom and inside the underlying rock joints (Fig. 2). The jet velocities were thereby at near-prototype scale, that is, up to 35 m/s. This guaranteed appropriate modelling of the turbulence and aeration conditions that govern a real plunge pool. The rock joints were simulated by a 1 mm-thick rectangular opening of one-or two-dimensional form inside a system of pre-stressed steel plates (Fig. 2).

For rock joints which may be considered as one-dimensional compared with the geometry of the jet at impact, that is, for a joint surface opening that is, at maximum, of the order of the jet diameter, the pressure fluctuations in the joints were governed by transient pressure waves. High peak pressures alternated with periods of low near-atmospheric pressure, especially for closed-end joints (Fig. 3). The pressure peaks were thus a multiple of the maximum pressures that were recorded at the plunge pool bottom. This non-linear transient behaviour of the pressures is caused by the significant compressibility of the air-water mixture entering the joint. When the jet excitation at the joint entrance has frequencies that are close to the fundamental resonance frequency of the joint, severe pressure amplifications may be generated.

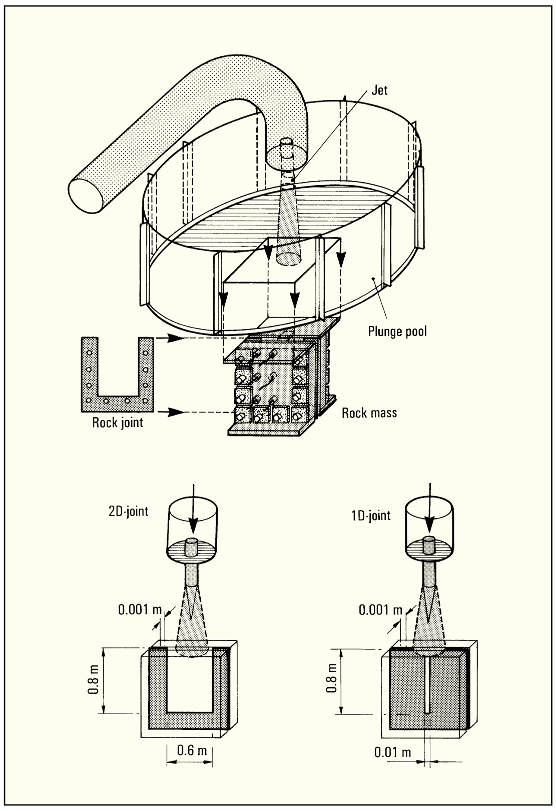

Fig. 2. View of the experimental installation and of 1D and 2D tested rock joints.

This is defined by the expression for the fundamental resonance frequency of a one-dimensional resonator volume. For example, for closed-end joints, this is written as:

$$f_{resonance} = \frac{c}{4 \cdot L_j} \qquad ...(1)$$

in which *c* stands for the pressure wave speed and L_j for the joint length.

Hence, as a function of the air content, which defines the compressibility and the wave speed *c* of the air-water mixture, and of the length of the joint, jet excitation frequencies may interact with the eigenfrequencies of the joints, resulting in severe pressure amplification effects. The wave speed thereby depends on sudden pressure changes in the joint: a high pressure results in a small air volume and high wave speed, whereas a low pressure results in high air contents and very small wave celerities.

Furthermore, a numerical model has been developed. This model simulates transient two-phase pressures in joints caused by a given fluctuating pressure signal at the joint entrance. It uses the 1D transient flow equations in conservative form and for a homogeneous air-water mixture. The wave speed *c* is computed as a function of the instantaneous pressure in the joint. Appropriate speed-pressure relationships were numerically calibrated, based on the experimental data. The computed pressures were in good agreement with the measured pressures. Both peak pressures and pressure spikes were appropriately generated by the numerical model.

As a result, dynamic pressures in joints may be described by a pressure amplification factor (describing the multiplication inside the joint of the pressures applied at the joint entrance) and by a frequency of occurrence of peak pressures. This concept is used and explained here for the scour model.

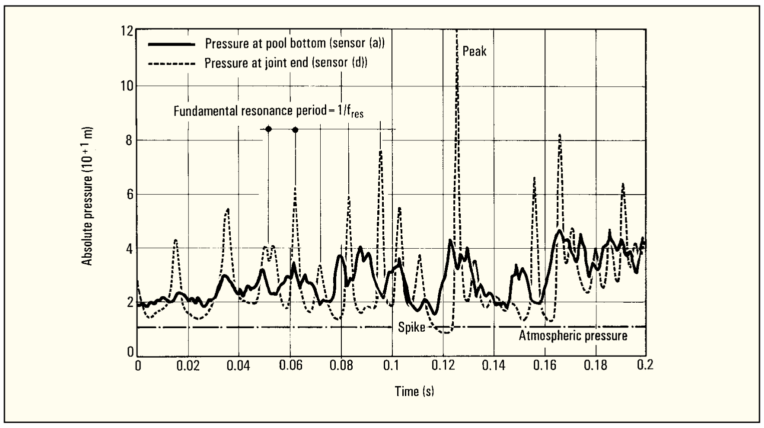

Fig. 3. Measured pressure signal at pool bottom and inside rock joint.

3. Comprehensive scour model

A comprehensive scour model was developed based on the experimentally and numerically investigated dynamic water pressures [Bollaert, 2002[1]]. The scour model comprises two methods which describe failure of jointed rock. The first one, the 'Comprehensive Fracture Mechanics' (CFM) method, determines the ultimate scour depth by expressing instantaneous or time-dependent joint propagation resulting from water pressures inside the joint. The second one, the 'Dynamic Impulsion' (DI) method, describes the ejection of rock blocks from their mass caused by sudden uplift pressures.

The structure of the comprehensive scour model consists of three modules: the falling jet, the plunge pool and the rock mass. The latter module implements the two previously mentioned failure criteria. Emphasis is given to the physical parameters necessary to describe the different processes accurately. The parameters are defined such that applications are easy to handle.

3.1. The module of the falling jet

This module describes how the hydraulic and geometric characteristics of the jet are transformed from dam issuance down to the plunge pool (Fig. 1). The parameters that characterize the jet at issuance are the velocity V_i, diameter (or width) D_i, issuance angle θ_i and the initial turbulence intensity Tu, defined as the ratio of velocity fluctuations to the mean velocity (2).

The jet trajectory is based on ballistics and air drag, and will not be outlined further. The jet module computes the longitudinal location of impact, the total trajectory length *L* and the velocity and core diameter at impact V_j and D_j. The turbulence intensity is presented below and defines the spread of the jet δ_{out} (3) [Ervine *et al.* 1997[3]]. Superposition of the outer spread to the initial jet diameter D_i results in the outer jet diameter D_{out}, which is used to determine the extent of the zone at the water-rock interface where severe pressure damage may occur. The relevant expressions are:

$$Tu = u' / U \qquad ...(2)$$

$$\frac{\delta_{out}}{X} = 0.38 \cdot Tu \qquad ...(3)$$

$$D_j = D_i \cdot \sqrt{\frac{V_i}{V_j}} \qquad ...(4)$$

$$V_j = \sqrt{V_i^2 + 2gZ} \qquad ...(5)$$

$$D_{out} = D_i + 2 \cdot \delta_{out} \cdot L \qquad ...(6)$$

in which δ_{out} is the half angle of outer spread, *X* the longitudinal distance from the point of issuance and *Z* the vertical fall distance of the jet. Typical outer angles of jet spread are 3-4 per cent for roughly turbulent jets. The corresponding inner angles of jet spread are 0.5 to 1 per cent [Ervine and Falvey, 1987[4]].

The angle of the jet at impact is not taken into account, which is reasonable for impingement angles that are close to the vertical (70-90°). For smaller impingement angles, it is proposed to redefine the water depth *Y* as the exact trajectory length of the jet through the water cushion, and not as the vertical difference between water level and pool bottom.

3.2.The module of the plunge pool

This module describes the hydraulic and geometric characteristics of the jet when traversing the plunge pool and defines the water pressures at the water-rock interface. The plunge pool water depth *Y* is essential. For near vertically impacting jets, it is defined as the difference between the water level and the bedrock level at the point of impact. The water depth increases with discharge and scour formation. Initially, *Y* equals the tailwater depth *h* (Fig. 1). During scour formation, *Y* has to be increased with the depth of the formed scour *t*. Prototype observations indicate possible mounding at the downstream end of the pool. This mounding results from detached rock blocks that are swept away and deposit immediately downstream. This can raise the tailwater level. The effect is not directly described in the model, but can easily be added to the computations by appropriate modification of the water depth during scour.

The water depth *Y* and jet diameter at impact D_j determine the ratio of water depth to jet diameter at impact Y/D_j. This ratio is directly related to jet diffusion. Caution should be taken when using this parameter. Significant differences may exist in practice because of the appearance of vortices or other surface disturbing effects, which can change the effective water depth in the pool. Engineering judgment is required on a case-by-case basis.

Dynamic pressures acting at the water-rock interface can be generated by core jet impact, appearing for small water depths *Y*, or by developed jet impact (shear layer), appearing for Y/D_j higher than 4 to 6 (for plunging jets), see Fig. 4. The most relevant pressure characteristics are the mean dynamic pressure coefficient C_{pa}, and the root-mean-square (rms) coefficient of the fluctuating dynamic pressures C'_{pa}, both measured directly under the centreline of the jet. These coefficients correspond to the ratio of pressure head (in metres) to incoming kinetic energy of the jet ($V^2/2g$) and are defined as follows:

$$C'_{pa} = 0.000215 \cdot \left(\frac{Y}{D_j}\right)^3 - 0.0079 \cdot \left(\frac{Y}{D_j}\right)^2 + 0.0716 \cdot \left(\frac{Y}{D_j}\right) + \eta \quad \text{for } \frac{Y}{D_j} \le 18 \qquad \text{...(7)}$$

$$C_{pa} = 38.4 \cdot (1 - \alpha_i) \cdot \left(\frac{D_j}{Y}\right)^2 \quad \text{for } Y/D_j > 4\text{-}6 \qquad \text{...(8)}$$

$$C_{pa} = 0.85 \qquad \text{for } Y/D_j < 4\text{-}6 \qquad \text{...(9)}$$

$$\alpha_i = \frac{\beta}{1+\beta} \qquad \text{...(10)}$$

Eqs.(8)-(10) are based on Ervine *et al*. [1997[3]]. The air concentration at jet impact α_i is defined as a function of the volumetric air-to-water ratio β. Plausible prototype values for β are 1-2. For a given α_i, mean and fluctuating dynamic pressures are defined as a function of *Y*, D_j and Tu. Similar expressions are proposed at locations radially outwards from the jet's centreline and can be found in Bollaert [2002[1]]. Tu is assumed to be representative for turbulent fluctuations and stability of the jet during its fall. Hence, Tu can be related to the rms values of the pressure fluctuations at the pool bottom. This is essential, because these fluctuations generate peak pressures inside underlying rock joints.

Following Eq.(7), the rms values of the pressure fluctuations at the pool bottom (C'_{pa}) depend on Y/D_j and Tu. The parameter η of Eq.(7) represents the degree of jet stability: η is equal to 0 for compact jets and goes up to 0.15 for highly turbulent and unstable jets. Compact jets (Tu < 1 per cent) are smooth during their fall, without any instability. Highly turbulent jets have a Tu > 5 per cent. In between, for 1 < Tu < 5 per cent, η has to be chosen between 0 and 0.15 as a function of jet stability and turbulence.

Generally, Tu is unknown. In such circumstances, an estimation can be made based on the type of outlet structure [Bollaert et al., 2002[5]]. However, Tu may largely depend on the outlet geometry, the flow pattern upstream, and so on. These aspects should be accounted for. As a first approximation, typical Tu values for high-velocity jets are 4 to 5 per cent.

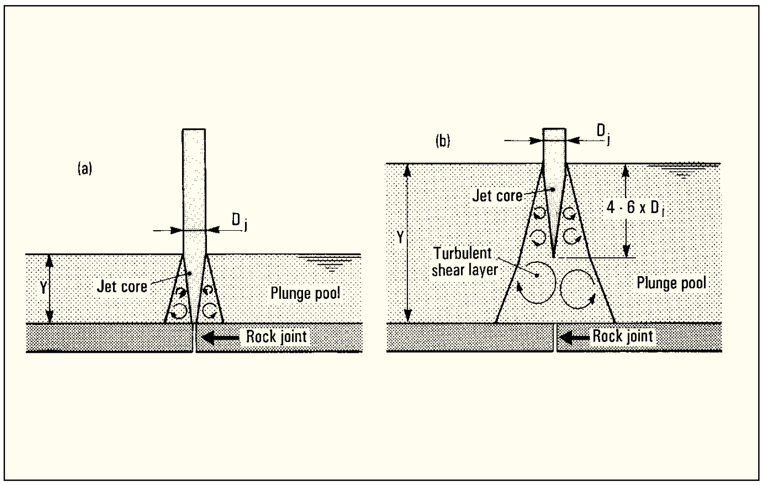

Fig. 4.Types of jet impact.

3.3 The module of the rock mass

The pressures defined at the bottom of the pool are used for determination of the transient pressures inside open-end or closed-end rock joints. The parameters are:

1. Maximum dynamic pressure coefficient : C^{max}_p
2. Characteristic amplitude of pressure cycles: Δp_c
3. Characteristic frequency of pressure cycles: f_c
4. Maximum dynamic impulsion coefficient : C^{max}_I

The first parameter is relevant to brittle propagation of closed-end rock joints. The second and third parameters express time-dependent propagation of closed-end rock joints. The fourth parameter is used to define dynamic uplift of rock blocks formed by open-end rock joints.

The maximum dynamic pressure C^{max}_p is obtained through multiplication of the rms pressure C'_{pa} with an amplification factor Γ^+, and by superposition with the mean dynamic pressure C_{pa}. Γ^+ expresses the ratio of the peak value inside the rock joint to the rms value of pressures at the pool bottom and has been determined experimentally:

$$\begin{aligned} \Gamma^+ &= \nu - 8 + 2 \cdot Y/D_j && \text{for } Y/D_j < 8 \\ \Gamma^+ &= \nu + && \text{for } 8 \leq Y/D_j \leq 10 \\ \Gamma^+ &= \nu + 28 - 2 \cdot Y/D_j && \text{for } 10 < Y/D_j \end{aligned} \quad ...(11)$$

in which ν is close to 0 for joints with several side branches or joints that are not tightly healed, and up to maximum 12 for tightly healed joints. The former joints were found to produce less significant pressure peaks, as a result of pressure diffusion and air dampening effects.

The product of C'_{pa} times Γ^+ results in a maximum pressure, written as:

$$P_{max}[\mathrm{Pa}] = \gamma \cdot C_p^{max} \cdot \frac{V_j^2}{2g} = \gamma \cdot (C_{pa} + \Gamma^+ \cdot C'_{pa}) \frac{V_j^2}{2g} \quad ...(12)$$

The main uncertainty of Eq.(12) lies in the Γ^+ factor, as previously defined in Eq.(11). It is interesting to note that, based on Eqs.(11)-(12), maximum pressures inside joints occur for Y/D_j ratios of between 8 and 10. This means that the most critical flood situation may not be the PMF, but rather the flow that results in a critical Y/D_j ratio.

The characteristic amplitude of the pressure cycles, Δp_c, is determined by the characteristic maximum and minimum pressures of the cycles. Minimum pressures are considered equal to the standard atmospheric pressure. Maximum pressures are chosen to be equal to the C^{max}_p value.

The characteristic frequency of the pressure cycles f_c follows the assumption of a perfect resonator system and depends on the air concentration in the joint α_i and on the length of the joint L_f. The air content inside the joints can be directly related to the air content at the plunge pool bottom [Bollaert, 2002[1]]. Its value depends on the velocity of the jet at impact and on the plunge pool depth. The joint length depends on the distances between the different joint sets. For practice, a first hand estimation for f_c is 25 to 100 Hz, considering a mean air-water wave speed of 200 to 400 m/s (depending on the mean pressure value) and joint lengths of about 1 m.

Beside the dynamic pressure inside rock joints, the resistance of the rock has to be determined. The cyclic character of the pressures generated by the impact of a high-velocity jet makes it possible to describe joint propagation by fatigue stresses occurring at the tip of the joint. This can be described by Linear Elastic Fracture Mechanics (LEFM), which handle both static and dynamic loadings and resistances by assuming a perfectly linear elastic, homogeneous and isotropic material. Despite these simplifying assumptions, their application to fractured rock becomes quite complicated when accounting for all relevant parameters [Atkinson, 1987[6]; Whittaker *et al.*, 1992[7]; Andreev, 1995[8]].

Therefore, a simplified methodology is proposed [Bollaert, 2002[1]]. The method represents a practical approach of the underlying theory and attempts to describe the main principles and parameters of influence such that engineering applications become plausible. It is called the Comprehensive Fracture Mechanics (CFM) method, and is applicable to any partially jointed rock. Pure tensile pressure loading inside rock joints is described by the stress intensity factor K_I. This parameter represents the amplitude of the rock mass stresses that are generated by the water pressures at the tip of the joint. The corresponding resistance of the rock mass against joint propagation is expressed by its fracture toughness K_{Ic}.

The issue is to obtain a comprehensive and physically correct implementation of the complex and dynamic situation encountered in fractured rock. Joint propagation distinguishes between brittle (or instantaneous) joint propagation and time-dependent joint propagation. The former happens for a stress intensity factor that is equal to or higher than the fracture toughness of the material. The latter occurs when the maximum possible water pressure results in a stress intensity which is inferior to the material's resistance. Joints may then be propagated by fatigue. Failure by fatigue depends on the frequency and the amplitude of the load cycles. The fracture mechanics implementation of the hydrodynamic loading consists of a transformation of the water pressures in the joints into stresses in the rock. These stresses are characterized by K_I as follows:

$$K_I = P_{max} \cdot F \cdot \sqrt{\pi \cdot L_f} \quad ...(13)$$

in which K_I is in MPa√m and P_{max} (12) in MPa. The implementation makes use of the following simplifying assumptions:

1. the dynamic character of the loading has no influence;
2. the water pressure distribution inside the joints is constant;
3. only simple geometrical configurations of rock joints are considered, and,
4. the joint surfaces are planar.

The boundary correction factor F depends on the type of crack and on its persistency, that is, its degree of cracking defined as a/B or b/W in Fig. 5. This figure presents three basic configurations for partially jointed rock. The choice of the most relevant geometry depends on the type and the degree of jointing of the rock. The first crack is of semi-elliptical or semi-circular shape and, pertaining to the applied water pressure, partially sustained by the surrounding rock mass in two horizontal directions. As such, it is the geometry with the highest possible support of the surrounding rock. Corresponding stress intensity factors should be used in the case of low to moderately jointed rock. The second crack is single-edge notched and of two-dimensional nature. Support from the surrounding rock mass is only exerted perpendicular to the plane of the notch and, as a result, stress intensity factors will be substantially higher than for the first case. Thus, it is appropri-

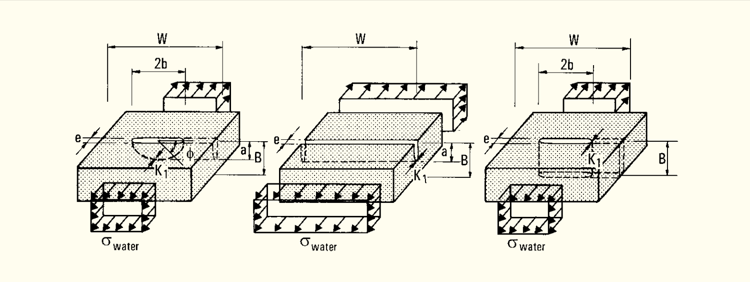

Fig. 5. Basic rock joint geometries.

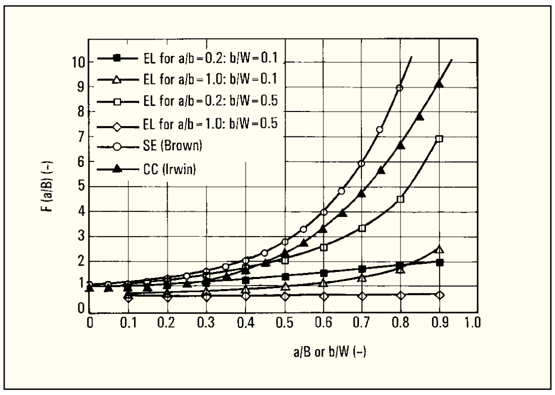

Fig. 6. F factor for degree of break-up of rock joints (EL = elliptical; SE = single-edge; CC = center-cracked).

ate for highly jointed rock. The third geometry is centre-cracked throughout the rock. Similar to the single-edge notch, only one-sided rock support can be accounted for. This support, however, is assumed to be slightly higher than for the single-edge notch. The second and third configurations are more sensitive to stresses and should rather be used for significantly to highly jointed rock.

A summary of F values is presented in Fig. 6. For practice, values of 0.5 or higher are considered to correspond to completely broken-up rock, that is, the DI method becomes more applicable than the CFM method. For values of 0.1 or less, it is believed that a pure tensile strength approach is more plausible rather than a fracture mechanics approach. However, most of the values in practice can be considered to be between 0.20 and 0.40, depending on the type and number of joint sets, the degree of weathering, joint interdistances, and so on. A first-hand broad-brush calibration of this parameter has been performed in Bollaert and Annandale [2004[9]] by comparison with Annandale's Erodibility Index Method [Annandale, 1995[10]]. Nevertheless, each study should be assessed on the basis of case-by-case judgment.

The fracture toughness K_{Ic} depends on a wide range of parameters. In the following, it has been related to the mineralogical type of rock and to the tensile strength *T* or the unconfined compressive strength UCS. Furthermore, corrections are made to account for the effects of the loading rate and the in-situ stress field of the rock mass The corrected fracture toughness is defined as the in-situ fracture toughness $K_{I,ins}$ and is based on a linear regression of available literature data. More detailed equations, as a function of the mineralogical rock composition, can be found in Bollaert [2002[1]].

$$K_{I\,ins,T} = (0.105 \text{ to } 0.132) \cdot T + (0.054 \cdot \sigma_c) + 0.5276 \qquad ...(14)$$

$$K_{I\,ins,UCS} = (0.008 \text{ to } 0.010) \cdot UCS + (0.054 \cdot \sigma_c) + 0.42 \qquad ...(15)$$

in which σ_c represents the confinement horizontal in-situ stress and T, UCS and σ_c are in MPa. Instantaneous joint propagation will occur if $K_I \geq K_{I,ins}$.

If this is not the case, joint propagation needs a certain time to happen. This is expressed by an equation as originally proposed to describe fatigue growth in metals:

$$\frac{dL_f}{dN} = C_r \cdot (\Delta K_I / K_{Ic})^{m_r} \qquad ...(16)$$

in which *N* is the number of pressure cycles. C_r and m_r are rock material parameters that are determined by fatigue tests and ΔK_I is the difference of maximum and minimum stress intensity factors at the joint tip.

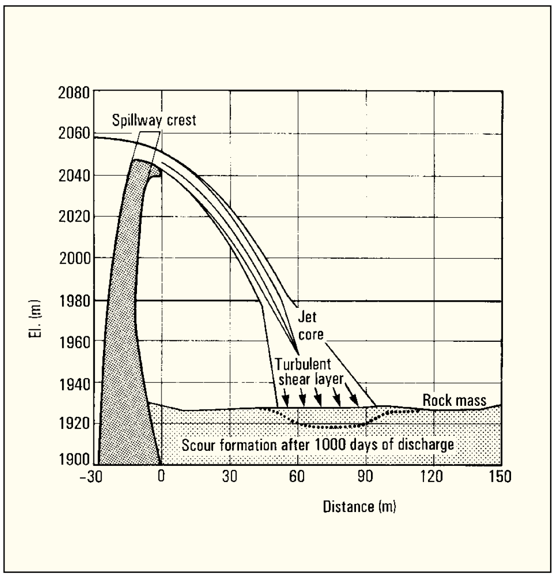

Fig. 7. Falling jet and plunge pool diffusion.

To implement time-dependent joint propagation into a comprehensive engineering model, m_r and C_r have to be known. They represent the vulnerability of rock to fatigue and have been derived from available literature data on the sensitivity of rock to quasi-steady break-up by water pressures in joints (= static fatigue) [Atkinson, 1987[6]].

Fig.8 summarizes m_r and C_r values for different types of rock. As such, m_r exponents may vary from 3 to 5 for marbles and sandstones, to 8 to 12 for other types of rock. It has to be emphasized that these values only express qualitative differences in sensitivity to scour and no absolute values. Hence, any application should be based on appropriate calibration. A first-hand calibration for granite resulted in $C_r = 10^{-7}$ for $m_r = 10$.

The fourth dynamic loading parameter is the maximum dynamic impulsion C^{max}_I in an open-end rock joint (underneath a single rock block), obtained by time integration of the net forces on the block (Newton):

$$I = \int_0^{\Delta tpulse} (F_u - F_o - G_b - F_{sh}) \cdot dt = m \cdot V_{\Delta tpulse} \qquad ...(17)$$

in which F_u and F_o are the forces under and over the block, G_b is the immerged weight of the block and F_{sh}

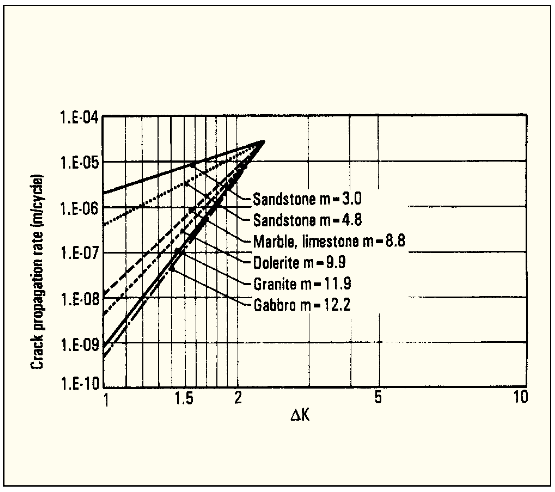

Fig.8. Qualitative crack propagation rate as a function of ΔK for different rock types.

represents the shear and interlocking forces. The shape of a block and the type of rock define the immerged weight of the block. The shear and interlocking forces depend on the joint pattern and the in-situ stresses. As a first approach, they can be neglected by assuming that progressive dislodgement and opening of the joints occurred during the break-up phase of the rock mass. The pressure field over the block is governed by the shear layer of the jet. The pressure field under the block corresponds to transient pressure waves.

Shear and interlocking forces depend on the contact-points between the blocks and the in-situ horizontal stress, and are difficult to assess. Also, pressure forces under the block may decrease because of block movement. As a first approximation, the pressures under the block are assumed to be independent of its movement.

The first step is to define the maximum net impulsion I^{max}. I^{max} is made non-dimensional by defining the impulse as the product of a net force and a time period. For this, the net force is first transformed into a pressure. This pressure can then be made non-dimensional by dividing it by the incoming kinetic energy $V^2/2g$. This results in a net uplift pressure coefficient C_{up}. The time period is non-dimensionalized by the travel period that is characteristic for pressure waves inside rock joints, ie, $T = 2 \cdot L_f/c$. This results in a time coefficient T_{up}. Hence, the non-dimensional impulsion coefficient C_I is defined by the product $C_{up} \cdot T_{up} = V^2 \cdot L/g \cdot c$ [m·s]. The maximum net impulsion I^{max} is obtained by multiplication of C_I by $V^2 \cdot L/g \cdot c$. The C_{up} value was measured close to 0.35. Analysis of uplift pressures resulted in the following expression for C_I :

$$C_I = 0.0035 \cdot \left(\frac{Y}{D_j}\right)^2 - 0.119 \cdot \left(\frac{Y}{D_j}\right) + 1.22 \qquad ...(18)$$

Failure of a rock block is expressed by the displacement it undergoes because of the net impulsion C_I. This is obtained by transformation of $V_{\Delta tpulse}$ Eq.(17) into a net uplift displacement h_{up} stating simply that:

$$V_{\Delta tpulse} = \sqrt{2g \cdot h_{up} \cdot} \qquad ...(19)$$

The net uplift displacement that is necessary to eject a rock block from its matrix is difficult to define. It depends on the protrusion and the degree of interlocking of the blocks. A tightly jointed rock will need a displacement that is equal to or higher than the height of the block. Less tightly jointed rock, or protruding rock, will be uplifted more easily. The necessary displacement is a model parameter that needs to be calibrated. A first-hand calibration of the Dynamic Impulsion (DI) method on Cahora Bassa dam [Bollaert, 2002[1]] resulted in a critical net uplift displacement of 0.2.

4. Application

The comprehensive scour model has been applied to an arch dam spillway design. The spillway consists of a central overflow, releasing a discharge of about 1000 m^3/s during PMF conditions. A downstream plunge pool water cushion of 50 m is formed during such floods, because of a tailpond dam.

The objective is to determine the ultimate scour depth and the probable time evolution of the phenomenon, to determine whether a concrete lining is necessary for the plunge pool. The main parameters of the falling jet and plunge pool modules are summarized in Table 1.

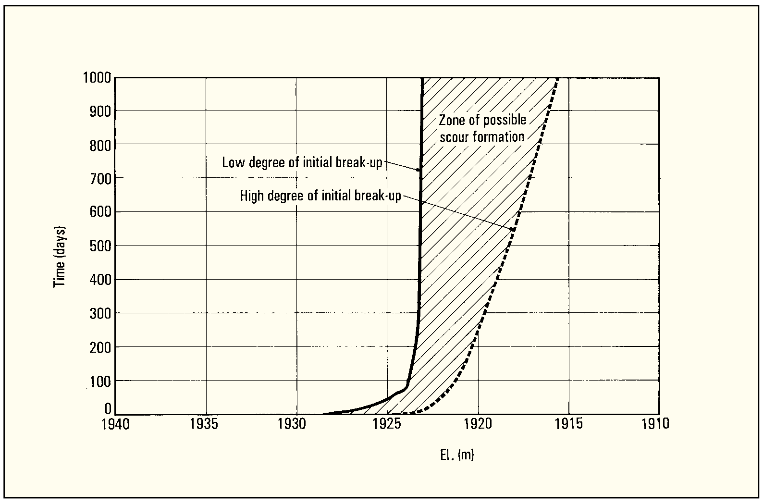

Fig. 9. Scour evolution based on CFM method.

The jet trajectory and plunge pool geometry are shown in Fig.7. The main rock mass characteristics are summarized in Table 2. The rock is considered to be good quality basalt, with an unconfined compressive strength of 150 MPa and a fracture toughness of 2.21 MPa. Two rock layers are distinguished, with a different initial degree of break-up of their joints.

Rock class II is located near the surface, while rock class I is situated further down into the rock mass and has less discontinuities (better quality rock).

Fig. 9 presents scour evolution as a function of time duration of the PMF discharge for a low and high initial degree of break-up of the different rock layers (Table 2). Tables 3 and 4 present the detailed results obtained by computing scour formation as a function of depth, based on the CFM and DI methods. The CFM method results in an ultimate scour depth of 1923 m a.s.l., while the DI method is somewhat deeper, that is, down to el. 1916.

Table 4 shows that, for a net uplift displacement h_{up} of between 0.2 and 0.5, the rock blocks are assumed to start moving and vibrating, without being necessarily ejected from their mass. Ejection is considered to start at h_{up} for values less than 0.20.

Table 1: Parameters of falling jet and plunge pool modules

Jet issuance from dam spillway			
Velocity	V_i	m/s	20
Equivalent diameter	D_i	m	7.20
Head difference	Z	m	88
Angle	θ_i	°	-35
Turbulence intensity	Tu_i	%	4
Jet impact in plunge pool			
Velocity	V_j	m/s	37
Air concentration	α_j	%	60
Aera of jet	A_j	m^2	10
Core diameter	D_j	m	3.66
Outer diameter	D_{out}	m	7.91
Angle of jet	θ_j	°	-70
Distance from dam toe	x	m	50
Jet impact at pool bottom			
Initial water depth	Y	m	50
Static pressure	C_{stat}	-	0.72
Mean dynamic pressure	C_{pa}	-	0.13
RMS dynamic pressure	C'_{pa}	-	0.24
Amplification factor	Γ^+	-	0

Table 2: Parameters of rock mass module

Parameter	Symbol	Class I	Class II	Unity
Unconf. Compr. Strength	UCS	150	150	MPa
Density rock	γ_r	2850	2850	kg/m^3
Typical joint length	L	1	1	m
Vertical persistence joint	P	0.25-0.40	0.35-0.50	-
Form of rock point	-	elliptical	elliptical	-
Tightness of joints	-	very closed	closed-open	-
Total number of joint sets	N_j	3	3	-
Typical rock block length	I_b	1	1	m
Typical rock block width	b_b	1	1	m
Typical rock block height	Z_b	0.7	0.7	m
Joint wave celerity	c	150	150	m/s
Fatigue sensibility	m	10	10	-
Fatigue coefficient	C	1.00E-08	1.00E-08	-

It is believed that, at a certain depth (> 10 m) in the rock mass, the CFM method is more applicable than the DI method, based on the statement that the joint network has not yet been completely formed. Hence, it may be concluded that future scour formation will occur relatively fast during the first 100 days of discharge. Further scour formation would need significantly more time. For a typical PMF duration estimated at only 20 days, the predicted maximum scour formation during the lifetime of the dam is estimated at 1920 m a.s.l. This depth is rather low and insignificant for the stability of the dam, the plunge pool and its sidewalls, and a plunge pool lining might be a too conservative design.

5. Conclusion

The comprehensive scour model evaluates the ultimate scour depth and the scour evolution in any type of jointed rock. The model is based on near-prototype measurements of dynamic pressure fluctuations at plunge pool bottoms and inside artificially created rock joints. Pressures in closed-end joints were found to be of cyclic character and have been assessed by their characteristic amplitude and frequency of occurrence. Pressures in open-end joints (underneath rock blocks) have been related to the corresponding rock surface pressures to define the net uplift impulsion on the blocks.

The model represents a comprehensive assessment of instantaneous and time-dependent (fatigue) fracturing of closed-end rock joints (CFM method) and of dynamic uplift of so formed rock blocks (DI method). The CFM method not only estimates the ultimate scour depth, but also the time evolution of the scour formation. Furthermore, both methods can also be applied outside of the jet's centreline at impact, which defines the spatial extent of the scour hole. In general, emphasis is placed on the physical parameters that are necessary to accurately describe the different phenomena. These parameters are defined in view of practical applications. This guarantees the comprehensive character of the model, without neglecting the underlying physical principles.

The application presented shows the promising and comprehensive character of the new model. Especially when past scour information is available, or when the relevant rock and hydraulic characteristics at the site are well known, it is believed that the model will be particularly useful to predict future scour formation as a function of time. Nevertheless, further calibration of the model parameters is necessary to enhance accuracy of the scour predictions. Its physical nature also makes it applicable to closely related engineering issues, such as uplift and/or cracking of concrete slabs of stilling slabs [Bollaert, 2003[11]], or break-up of fractured coastal structures by violent wave impact. ◊

Table 3: Scour formation as a function of time based on Comprehensive Fracture Mechanics (CFM) method

CLASS	JET IMPACT			STRESS INTENSITY KL				FRACTURE TOUGHNESS K_{Ic}				TIME DEPENDENCY		
	El.	Type jet	Y/D	C_{stat}	C_{pa}	C'_{pa}	K_I	UCS	K_{Ixy}	Propagation	El.	T	T	Total T
	(m a.s.l.)	-	-	-	-	-	(MPa.m$^{0.5}$)	(MPa.m$^{0.5}$)		-	(m.a.s.l.)	(h)	(days)	(days)
II	1928.8	developed	10.2	0.72	0.13	0.24	2.25257	150	2.21	brittle	1928.8	0.00E+00	0.00E+00	inst
II	1927.6	developed	10.5	0.73	0.12	0.23	2.12619	150	2.21	fatigue	1927.6	2.70E+02	1.13E+01	1.92E+01
II	1927.0	developed	10.6	0.74	0.12	0.23	2.06466	150	2.21	fatigue	1927.0	3.86E+02	1.61E+01	3.53E+01
II	1925.8	developed	10.8	0.76	0.11	0.22	1.94509	150	2.21	fatigue	1925.8	7.93E+02	3.31E+01	9.13E+01
II	1924.5	developed	11.1	0.78	0.11	0.22	1.83037	150	2.21	fatigue	1924.5	1.65E+03	6.89E+01	2.08E+02
II	1923.9	developed	11.2	0.79	0.11	0.21	1.7749	150	2.21	fatigue	1923.9	2.40E+03	1.00E+02	3.08E+02
I	1923.3	developed	11.3	0.80	0.10	0.21	1.48914	150	2.21	fatigue	1923.3	1.98E+04	8.24E+02	1.13E+03
I	1922.7	developed	11.5	0.81	0.10	0.21	1.0911	150	2.21	end	1922.7	8.29E+05	3.45E+04	3.57E+04
I	1922.0	developed	11.6	0.81	0.10	0.20	1.05738	150	2.21	end	1922.0	1.21E+06	5.05E+04	8.61E+04

Table 4: Ultimate scour depth based on Dynamic Impulsion (DI) method

CLASS	JET IMPACT			DYNAMIC IMPULSION											
	El.	Type jet	Y/D_j	CP	CT	CI	Imax	Gb	Time	Inet	V_{up}	h_{up}	h_{up}/z	Uplift	El.
	(m.a.s.l.)	-	-	-	-	-	(Ns)	(kg/m^2)	(s)	(Ns)	(m/s)	(m)	-	-	(m.a.s.l.)
II	1928.8	intact	10.4	0.30	1.50	0.36	4986	1295	0.072	3461	2.67	0.36	0.52	uplift	1928.8
II	1925.1	intact	11.1	0.30	1.50	0.33	4533	1295	0.072	3009	2.32	0.28	0.39	vibrations	1925.1
II	1923.9	intact	11.4	0.30	1.50	0.32	4395	1295	0.072	2870	2.22	0.25	0.36	vibrations	1923.9
I	1923.3	intact	11.5	0.30	1.50	0.31	4314	1295	0.072	2790	2.15	0.24	0.34	vibrations	1923.3
I	1920.8	intact	12.0	0.30	1.50	0.30	4062	1295	0.072	2538	1.96	0.20	0.28	vibrations	1920.8
I	1918.3	intact	12.5	0.30	1.50	0.28	3834	1295	0.072	2310	1.78	0.16	0.23	vibrations	1918.3
I	1915.9	intact	13.0	0.30	1.50	0.26	3630	1295	0.072	2105	1.63	0.13	0.19	stability	1915.9
I	1913.4	intact	13.6	0.30	1.50	0.25	3433	1295	0.072	1909	1.47	0.11	0.16	stability	1913.4
I	1912.2	intact	13.8	0.30	1.50	0.24	3353	1295	0.072	1829	1.41	0.10	0.15	stability	1912.2

Acknowledgments

The experimental and numerical modelling of dynamic pressures has been done by the author at the Laboratory of Hydraulic Constructions of the Swiss Federal Institute of Technology, Lausanne, Switzerland, under the supervision of Prof. A. Schleiss. Financial support has been provided by the Swiss Committee of Dams and by Stucky, within the framework of the CTI.

References

1. **Bollaert, E.,** "Transient water pressures in joints and formation of scour due to high-velocity jet impact", Communication 13, Laboratory of Hydraulic Constructions, Lausanne, Switzerland; 2002.
2. **Bollaert, E. and Schleiss, A.**, "Scour of rock due to the impact of high-velocity jets. Part II: Experimental results of dynamic pressures at pool bottoms and in one- and two-dimensional closed end rock joints", Journal of Hydraulic Research, IAHR, Vol. 41, No.5, pp.465-480, 2003.
3. **Ervine, D.A., Falvey, H.T., and Withers, W**. "Pressure fluctuations on plunge pool floors", *Journal of Hydraulic Research*, Vol. 35, No. 2,; 1997.
4. **Ervine, D.A. and Falvey, H.R.**, "Behaviour of turbulent jets in the atmosphere and in plunge pools", Proceedings of the Institution of Civil Engineers. Part 2, Vol. 83, 1987.
5. **Bollaert, E., Falvey, H.T., and Schleiss, A.**, "Turbulent jet impingement in plunge pools: the particular characteristics of a near-prototype physical model study", Proceedings of Riverflow 2002, Louvain-la-Neuve, Belgium, 2002.
6. **Atkinson, B.K.**, "Fracture Mechanics of Rock", Academic Press Inc., London, UK; 1987.
7. **Whittaker, B.N., Singh, R.N. and Sun, G.,** "Rock Fracture Mechanics" Elsevier publishers. The Netherlands; 1992.
8. **Andreev, G.E.,** "Brittle Failure of Rock Materials." Balkema, Rotterdam, Brookfield; 1995.
9. **Bollaert, E. and Annandale, G.**, "Parametric Comparison of Comprehensive Scour Model and Erodability Index Method," submitted to the International Conference on Hydraulics of Dams and River Structures, Tehran, Iran, 26-28 April 2004.
10. **Annandale, G.**, "Erodibility", Journal of Hydraulic Research, IAHR, Vol. 33, No.4, pp.471-494, 1995.
11. **Bollaert, E.,** "The influence of joint aeration on dynamic uplift of concrete slabs of plunge pool linings", XXX IAHR Conference, Thessaloniki, Greece; August 2003.

E. Bollaert

Erik Bollaert, PhD, is President of AquaVision Engineering Ltd., a company working in the field of interactive hydraulic-geotechnic-environmental engineering, such as scour behind hydraulic structures. He has been involved in engineering projects worldwide for almost 10 years (USA, Iran, Iceland, Bolivia, France, Switzerland). He elaborated his PhD in the field of rock scour due to high-velocity jet impact. Erik Bollaert co-organized the "International Workshop on Rock Scour" in Lausanne (EPFL) and is one of the editors of the book "Rock Scour due to falling high-velocity jets", published in 2002 (Swets & Zeitlinger, The Netherlands). He is also Senior Research Associate at the Laboratory of Hydraulic Constructions of the Swiss Federal Institute of Technology in Lausanne.

AquaVision Engineering Ltd., Chemin des Champs - Courbes 1, CH-1024 Ecublens, Switzerland.